Proceedings of the 2025 SICE Festival with Annual Conference
September 9-12, 2025, Chiang Mai, Thailand

Noise Reduction by Zero-Phase Filter in Infrasound Observation Using MEMS Atmospheric Pressure Sensor

Genki Shimizu[1†], Yoshiyuki Noda[2] and Momoko Kojima[3]

[1]Integrated Graduate School of Medicine, Engineering and Agricultural Sciences, University of Yamanashi, Kofu, Yamanashi, Japan
(E-mail: g24tm014@yamanashi.ac.jp)
[2]Graduate Faculty of Interdisciplinary, University of Yamanashi, Yamanashi, Japan
(Tel: +81-55-220-8440; E-mail: noday@yamanashi.ac.jp)
[3]National Metrology Institute of Japan, AIST, Ibaraki, Japan

Abstract: This study is concerned with an advanced noise reduction approach for an infrasound observation system using a Micro-Electro-Mechanical Systems (MEMS) atmospheric pressure sensor. The infrasound is defined as atmospheric acoustic waves with frequencies lower than 20 Hz which are in an inaudible range of the human ear, and is excited by natural phenomena such as volcanic eruptions and tsunamis. In recent years, the MEMS atmospheric pressure sensor has been used for realizing multipoint observation of the infrasound. However, the noise ratio of the MEMS pressure sensor is higher than that of the dedicated sensor. In this study, we propose the noise reduction approach using a Finite-Impulse-Response type Zero-Phase Filter (FIR-ZPF) for visualizing clearly the infrasound. In the acceptable short time batch processing for updating the infrasound observation data, the FIR-ZPF is useful to the noise reduction with no phase delay. The efficacy of the proposed noise reduction approach is verified by the experiments with the lifting device for generating the artificial pressure variations. The three type MEMS atmospheric pressure sensors are installed into the lifting device. It was shown that the proposed approach using the FIR-ZPF enables to show precisely and clearly the trend of the atmospheric pressure sensor signal with suppressing the noise.

Keywords: infrasound, MEMS atomospheric pressure sensor, filter, noise reduction, signal processing

1. INTRODUCTION

It is known that global-scale natural phenomena, such as tsunamis, volcanic eruptions, and lightning, generate acoustic waves called infrasound at the time of occurrence [1]. The infrasound is defined as atmospheric acoustic waves with frequencies lower than the audible range of the human ear [2]. Since the human audible frequency range is generally from 20 Hz to 20 kHz, the upper frequency limitation of the infrasound is approximately 20 Hz. Due to its long wavelength and low attenuation caused by air molecule viscosity, the infrasound can propagate over thousands of kilometers through the atmosphere and has been used as a remote sensing tool for volcanic eruptions and nuclear tests [3]. In recent years, research on the generation mechanisms and propagation characteristics of infrasound caused by earthquakes and tsunamis has also advanced, and its application for early disaster detection is expected [4][5].

A major issue in infrasound observation is the presence of significant noise within the signal of interest. In [6], it has been reported that the infrasound detection at the Lutzow-Holm Bay in Antarctica is difficult by the noise occurred by the strong winds. Thus, the noise reduction method in which the porous hoses are connected to the detector has been proposed. However, it has the problems that the large area is needed for implementing the hoses and the performance of the infrasound detection method can be influenced by the prous hose structure such as the volume and number of the inlet. In [7], Dai, *et al.* pointed out the significant influence of noise components in infrasound signals and proposed the MCWGCC-NMF method, which combines spatial and frequency domain information. This method attempts to extract the signal components using non-negative matrix factorization and generalized cross-correlation, and remove noise using mask weighting. However, it has been noted that when the frequency components of the signal and noise overlap, misclassification of components tends to occur, and it is especially limited in suppressing low-frequency noise. Furthermore, the disaster can be detected precisely by spreading widely the sensors for observing the infrasound. However, since dedicated sensors for the infrasound are expensive, it is difficult that a lot of the sensors are located on the wide area. Therefore, utilization of Micro-Electro-Mechanical Systems (MEMS) atmospheric pressure sensors is promoted for observing the infrasound [8]. The MEMS pressure sensors are reasonable and expected to be useful for multipoint installation and large-scale observation networks. However, the MEMS pressure sensor tends to display a lower performance than the dedicated sensor for the infrasound. The noise ratio of the MEMS pressure sensor is especially higher than that of the dedicated sensor.

In this study, we propose the noise reduction approach of the MEMS atmospheric pressure sensor for the infrasound observation. In general, a Infinite-Impulse-Response type Low-Pass Filter (IIR-LPF) is used to reduce the noise on the sensing signal. In the infrasound observation, it is, however, difficult to confirm accurately the occurrence time of disaster from the signal processed by IIR-LPF because of phase delay caused by IIR-LPF.

† Genki Shimizu is the presenter of this paper.

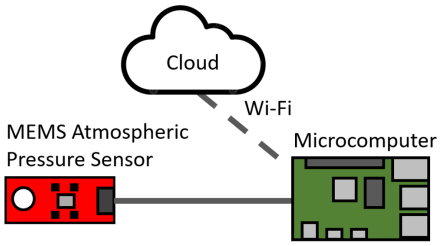

Fig. 1: Infrasound observation system using MEMS atmospheric pressure sensor

Therefore, we assume that short-time batch processing is acceptable for observing the infrasound, since the target frequency range of the infrasound observation is much lower than the sampling frequency of the MEMS sensor. In this assumption, a Finite-Impulse-Response type Zero-Phase Filter (FIR-ZPF) can be applied for the noise reduction of the sensing signal by the MEMS pressure sensor. The efficacy of the proposed approach is verified by implementing to MEMS pressure sensors installed into the lifting device. Moreover, the proposed approach is applied to three type MEMS atmospheric pressure sensors for the comparative verification of sensors performance.

2. INFRASOUND OBSERVATION SYSTEM USING MEMS ATMOSPHERIC PRESSURE SENSOR

The system configuration of the infrasound observation system in this study is shown in Fig. 1. In this system, the atmospheric pressure can be detected by the MEMS sensor, and the sensor signal is processed in the microcomputer for reducing the noise in the signal and sending the processed data to a cloud platform for infrasound analysis though a Wi-Fi network. The sampling time of the atmospheric pressure is 10 millisecond. In the microcomputer, batch processing is performed, and the processed data is sent to the cloud platform every a few hundred milliseconds.

3. NOISE REDUCTION BY FIR-ZPF

One of ideal low-pass filter is a Zero-Phase Filter (ZPF) which has no phase delay and enables to reduce adequately noise over a cut-off frequency. The ZPF on frequency domain can be represented as

$$H(\omega) = \begin{cases} 1, & (|\omega| \leq \omega_c), \\ 0, & (|\omega| > \omega_c), \end{cases} \tag{1}$$

where ω is the angular frequency and ω_c is the cut-off angular frequency. Since the ZPF in Eq. (1) consists of real numbers on frequency domain, it does not have the phase delay. Moreover, the noise over the cut-off frequency can be dampen completely by applying the ZPF. By performing the inverse Fourier transform to Eq. (1), we can derive the ZPF on time domain as

$$h(\tau) = \frac{1}{2\pi}\int_{-\omega_c}^{\omega_c} 1 \cdot e^{i\omega\tau}\, d\omega = \begin{cases} \frac{\sin(\omega_c\tau)}{\pi\tau}, & (\tau \neq 0), \\ \frac{\omega_c}{\pi}, & (\tau = 0), \end{cases} \tag{2}$$

where τ is the time based on the target time τ_{tg} as $\tau = t - t_{\mathrm{tg}}$. The ZPF can be represented by a sinc function on the time domain. The sinc function in Eq. (2) can be approximated with discrete time as

$$h(\kappa) = \begin{cases} \frac{\sin(\omega_c T_s \kappa)}{\pi T_s \kappa}, & (\kappa \neq 0), \\ \frac{\omega_c}{\pi}, & (\kappa = 0), \end{cases} \tag{3}$$

where κ is the sampling number based on the target time, and T_s is the sampling time. For implementing the discrete-time sinc function in Eq. (3) to the microcomputer, the window function with the width $-\kappa_w/2 \leq \kappa \leq \kappa_w/2$ is set to Eq. (3). In the case of applying the window function, the ripple on the frequency domain can be caused by discontinuities on the edges of the window function. Therefore, we provide a hann window as the window function as

$$w(\kappa) = \begin{cases} 0.5\left(1 - \cos\left(\frac{2\pi\left(\kappa + \frac{\kappa_w}{2}\right)}{\kappa_w}\right)\right), & (|\kappa| \leq \kappa_w), \\ 0, & (|\kappa| > \kappa_w). \end{cases} \tag{4}$$

The FIR-ZPF can be realized by convolving the sensor signal with the sinc and the window functions as

$$p_f(k_{tg}) = \sum_{\kappa=-\kappa_w/2}^{\kappa_w/2} h(\kappa)\, w(\kappa)\, p_s(\kappa + k_{tg}). \tag{5}$$

where p_f is the processed data by the FIR-ZPF, and p_s is the original sensor signal from the MEMS sensor. k_{tg} is the sampling number at the target time, that is $t_{tg} = k_{tg}T_s$. The overview of the FIR-ZPF is shown in Fig. 2. In the FIR-ZPF, the sinc function with the hann window is spanned within the window centered at the target time t_{tg}. In the case that the time span of the window is within that of the batch process, the FIR-ZPF derived in this study can be performed, and the noise over the cut-off frequency in the sensor signal can be reduced with no phase delay.

In addition, if it is required to perform a Finite-Impluse-Response type Low-Pass Filter (FIR-LPF) in real time, the target time is set to the present time and the following convolution can be performed:

$$p_f(k_{tg}) = \sum_{\kappa=-\kappa_w/2}^{\kappa_w/2} h(\kappa)\, w(\kappa)\, p_s\left(k_{tg} - \frac{\kappa_w}{2} + \kappa\right). \tag{6}$$

Therefore, a time delay $\kappa_w/2$ is occurred in the FIR-LPF.

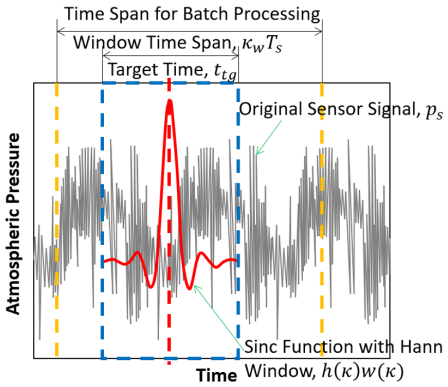

Fig. 2: Infrasound observation system using MEMS atmospheric pressure sensor

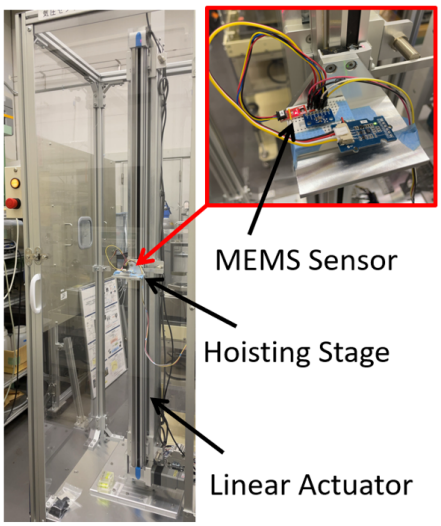

Fig. 3: Experimetal apparatus

4. EXPERIMENTAL VERIFICATION

The efficacy of the proposed noise reduction approach using the FIR-ZPF is verified by the experiments with the three-type MEMS atmospheric pressure sensors, BME280(Bosch) [9], BMP581(Bosch) [10] and DPS310(Infineon) [11]. The specifications of the MEMS sensors are shown in Table. 1. In the experiments, the MEMS sensors are moved vertically by the linear actuator as shown in Fig. 3. The variation of the infrasound can be simulated by moving vertically using the linear actuator. The MEMS sensors are fitted to the lifting stage on the linear actuator. The artificial pressure variations with the frequency 1 Hz are produced in the experiments. And, the total amplitudes of the pressure variations are set as 10 Pa and 5 Pa. The experimental results are shown in Fig. 4. The graphs from (a) to (c) in Fig. 4 show the results in the experiments with the total amplitude 10 Pa of the pressure variations. The graphs from (d) to (f) show those with the total amplitude 5 Pa. The graphs (a) and (d), the graphs (b) and (e) and the graphs (c) and (f) are the results of BME280, BMP581 and DPS310, respectively. The black, the green, the yellow and the red lines are the original sensor signals, the data processed by the IIR-LPF, the FIR-LPF and the FIR-ZPF, respectively. In the all filters, the cut-off frequency is given as 1.5 Hz. In the FIR-LPF and the FIR-ZPF, the time span of the hann window is 0.2 seconds.

The results of the IIR-LPF have the lowest responses in the all sensors in this study. The results of the FIR-LPF have the longest delay in the all sensors. The processed data by the FIR-ZPF enables to show precisely the trend of the sensor signal with suppressing the noise. The total amplitudes of the all sensors are slightly larger than the setting parameter of the total amplitude. It is due to inertia influence in the vertical motion of the sensors.

Furthermore, we perform the comparative verification of the three-types MEMS atmospheric pressure sensors with the FIR-ZPF processing. In order to reduce the inertia influence in the sensor motion, the lifting stage is moved with a trapezoidal curve designed to produce the pressure variation of ± 5 Pa. The experimental results are shown in Fig. 5. The graphs (a), (b) and (c) show the results of BME280, BMP581 and DPS310, respectively. The black and the red lines are the original sensor signal and the data processed by the FIR-ZPF, respectively. The result of DPS310 indicates precisely the setting maximum pressure. Therefore, it was confirmed that the atmospheric pressure can be detected precisely by DPS310 with the noise reduction using the FIR-ZPF.

5. CONCLUSION

In this study, we proposed the noise reduction approach using the FIR-ZPF in the infrasound observation system using the MEMS atmospheric pressure sensor. In the acceptable short time batch processing for updating the infrasound observation data, the FIR-ZPF is useful to the noise reduction with no phase delay. In the experimental verification, it was confirmed that the pressure data processed by the FIR-ZPF enables to show precisely the trend of the atmospheric pressure sensor signal with suppressing the noise. Furthermore, the low-frequency atmospheric pressure can be visualized clearly by DPS310, which is a capacitance-type MEMS sensor, with the noise reduction approach using the FIR-ZPF.

REFERENCES

[1] M. Yamamoto, "Current Status of Infrasound Research in Japan and Abroad", *Monthly Journal Chikyu*, Vol. 34, No. 10, pp. 554–559, 2012.

[2] Makoto Tahira, "Measurement and Propagation of Infrasound", *Journal of the Acoustical Society of Japan*, Vol. 63, No. 8, pp. 428–433, 2007.

[3] Yuji Saito, "A study of infrasound observation using MEMS atmospheric pressure sensor", *Tohoku University Bulletin of Communication and Electrical Engineering Discussions*, Vol. 87, No. 1, pp. 292–293, 2018.

[4] J. Paul Mutschlecner and Rodney W. Whitaker, "Infrasound from earthquakes", *Journal of*

Table 1: Specifications of evaluated MEMS pressure sensors.

Model	Manufacturer	Type	Meas. range (kPa)	Resolution (Pa)	Abs. accuracy (Pa)	Rel. accuracy (Pa)	Meas. noise (Pa)	Temp. coeff. (Pa/K)
BME280[9]	Bosch	Piezoresistive	30–126	0.18	±100	±12	0.2	±1.5
BMP581[10]	Bosch	Capacitive	30–125	0.016	±30	±6	0.08	±0.5
DPS310[11]	Infineon	Capacitive	30–120	0.06	±100	±6	0.2	±0.5

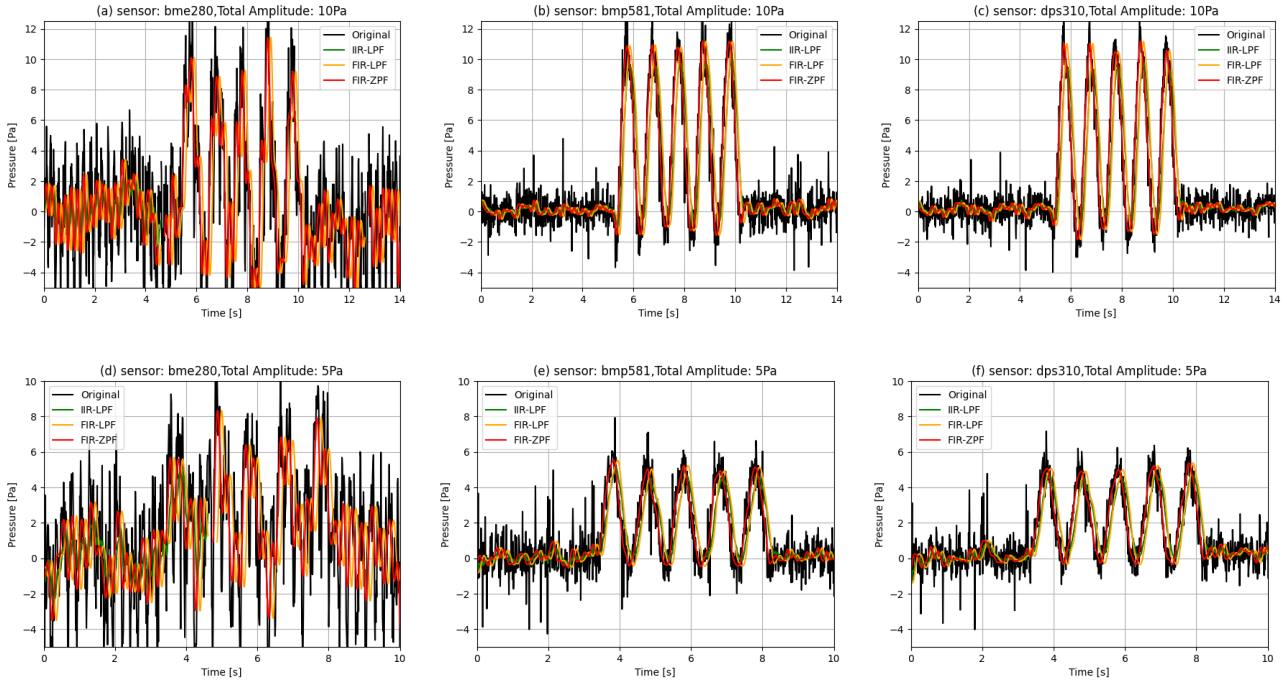

Fig. 4: Experimental results of atmospheric pressure detection by three-type MEMS sensors in artificial pressure variation using linear actuator.

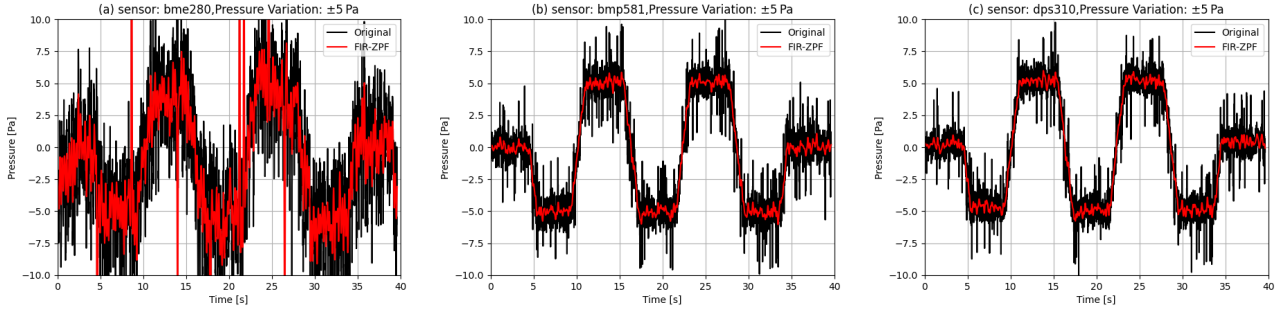

Fig. 5: Experimental results of atmospheric pressure detection by three-type MEMS sensors in artificial pressure variation with trapezoidal curve

Geophysical Research, Vol. 110, D01108, doi.org/10.1029/2004JD005067, 2005.

[5] Masayuki Yamamoto, "Understanding tsunami scale by infrasound monitoring network on land", *Journal of Industry-Academia-Government Collaboration*, Vol. 16, No. 2, pp. 7–9, 2020.

[6] M. Kanao, *et al.*, "Detection of infrasound sources using three-years array data in 2019–2021 deployed at the Lützow-Holm Bay region, Antarctica", *Annals of Geophysics*, Vol. 67, No. 5, A554, 2024.

[7] Yijing Dai, *et al.*, "Noise reduction in infrasound signals based on mask coefficient binary weighting – Generalized cross correlation – Non – negative matrix factorization algorithm", *Journal of Applied Acoustics*, Vol. 186, No. 5, 2022.

[8] Momoko Kojima, "Characteristics Evaluation of MEMS Atmosheric Pressure Sensors", Measurement: Sensors, doi.org/10.1016/j.measen.2024.101679, 2024.

[9] Bosch,BME280 datasheet,Online,https://www.bosch-sensortec.com/media/boschsensortec/downloads/datasheets/bst-bme280-ds002.pdf,2025,(Accessed 16 April 2025).

[10] Bosch,BMP581 datasheet,Online,https://www.bosch-sensortec.com/media/boschsensortec/downloads/datasheets/bst-bmp581-ds004.pdf,2025,(Accessed 16 April 2025).

[11] Bosch,BMP581 datasheet,Online,https://www.bosch-sensortec.com/media/boschsensortec/downloads/datasheets/bst-bmp581-ds004.pdf,2025,(Accessed 16 April 2025).